A Scalable Approach to the Assessment of Storm Impact in Distributed Automation Power Grids

Alberto Avritzer[1], Laura Carnevali[4], Lucia Happe[3], Anne Koziolek[3], Daniel Sadoc Menasche[2], Marco Paolieri[4], and Sindhu Suresh[1]

[1] Siemens Corporation, Corporate Technology, Princeton, USA
[2] Federal University of Rio de Janeiro, Rio de Janeiro (UFRJ), Brazil
[3] Karlsruhe Institute of Technology (KIT), Germany
[4] University of Florence, Florence, Italy

Abstract. We present models and metrics for the survivability assessment of distribution power grid networks accounting for the impact of multiple failures due to large storms. The analytical models used to compute the proposed metrics are built on top of three design principles: state space factorization, state aggregation, and initial state conditioning. Using these principles, we build scalable models that are amenable to analytical treatment and efficient numerical solution. Our models capture the impact of using reclosers and tie switches to enable faster service restoration after large storms. We have evaluated the presented models using data from a real power distribution grid impacted by a large storm: Hurricane Sandy. Our empirical results demonstrate that our models are able to efficiently evaluate the impact of storm hardening investment alternatives on customer affecting metrics such as the expected energy not supplied until complete system recovery.

Keywords: Survivability, cyber-physical systems, smart-grid.

1 Introduction

In this paper, we introduce a new approach to the modeling and analysis of large power distribution networks, with the goal of supporting the evaluation of investment alternatives for storm hardening of overhead transmission facilities. Specifically, the focus of this work is on the modeling and analysis of US Northeast power distribution network outages that result from mid-Atlantic hurricanes and tropical storms.

Hurricane Sandy hit the US northeast overhead power distribution network with strong winds on October 29 and 30, 2012. The impact on the overhead power network in New York City and Westchester county was so severe that about 70% of the 868,347 non-network customers (i.e., customers served by overhead lines) in these areas were interrupted. In Westchester county alone 320,926 customer outages were reported [11]. The total number of interruptions of non-network customers in the Con Edison territory was 1,115,294. These customer outages were a consequence of the loss of nearly 1,000 utility poles and over 900 transformers. In the Bronx/Westchester area, 699 poles and 718 transformers were replaced [11]. One of the most important reported causes of these customer outages in Westchester county was the fall-down of trees and branches due to the co-habitation of power distribution with Westchester county's forests [26]. Therefore, over 1,000 roads in Westchester county were blocked by trees and branches after Hurricane Sandy.

As a result of the damage to overhead power distribution network caused by Hurricane Sandy, a study was commissioned by the City of New York to assess the feasibility of undergrounding parts of the overhead network [27]. The total cost of replacement of the overhead network in the Bronx/Westchester county is estimated at $27.2 billion. A total replacement covering all of New York City and Westchester county is estimated at $42.9 billion. In [12] a list of the storm hardening initiatives for the electric overhead distribution system was presented. These initiatives include, among others, the use of additional reclosers and sectionalizer switches, tree trimming, and selective undergrounding [12].

The utility uses a coarse grained risk model to identify the relationship between the required capital investment for storm hardening of a specific asset and the risk reduction achieved in terms of asset outage durations using wind damage probabilities [12]. Unfortunately, the coarse grain risk assessment approach is not detailed enough to assess the customer impact of large storms. The risk assessment approach used by the utility can be improved by using a metric that captures the evolution of the repair process (both automated

and manual), and the energy not supplied from the start of the outage event to the completion of all required repairs. Therefore, there is a need to improve the utility risk prioritization of storm hardening investment approaches by modeling the impact of sectionalizing, undergrounding, and tree trimming on a metric of interest to the utility. We call this metric the *customer affecting metric*. In this paper, the customer affecting metric used is the *average energy not supplied from the time of the emergency to full restoration of service to all customers*. The level of accuracy required in the power grid model needs to be sufficient to compare design alternatives; the model has to be accurate enough to properly distinguish between the investment options.

We model the impact of using reclosers and tie switches to enable faster service restoration after large storms. The use of reclosers and tie switches provides the following benefits to the power utility: (1) enables sectionalization of customers reducing the impact of outages, (2) reduces the number of energized down wires, and (3) enables the automated and remote reconfiguration of the overhead distribution network during the several phases of the storm emergency (preparation and restoration) [11].

Survivability is the ability of the system to continue functioning during and after a failure or disturbance event [18]. In our previous work, we developed survivability models accounting for single failures in distribution automation power grids [21,24,1]. The analytical models used to compute the proposed metrics are built on top of three design principles: state space factorization, state aggregation, and initial state conditioning. In [2], we extended the survivability model to account for multiple-failures.

The main contributions of this paper are the following.

- A *scalable model* to assess survivability related metrics of smart power-grids. The model allows us to efficiently compute survivability related metrics in networks consisting of hundreds of loops. The model captures the smart-grid/cyber-physical interconnection as well as automatic restoration/manual restoration, and allows for general distributions for the automatic and manual restoration, adopting recently proposed techniques of non-Markovian analysis.
- A *characterization of hurricanes*, which accounts for historical data and can make use of geographical information. Each hurricane is characterized by a hurricane model, which indicates the wind strength in knots at each section of the grid. The hurricane model is then used to obtain a global survivability related metric for the whole network as a function of the network topology and the hurricane pattern.
- *What-if analysis*, which allows to quickly identify the impact of different strategies for power grid storm hardening, such as distributed generation, tree trimming, and moving lines underground. This analysis can be used for planning and optimization purposes.

We illustrate the practicality of our approach by evaluating the impact of Hurricane Sandy on a model of a overhead distribution network of the scale of the Con Edison overhead distribution network in New York, which serves the areas of Staten Island, the Bronx, Brooklyn, Queens, and Westchester county.

The remainder of this paper is organized as follows. In Section 2, we describe the cyber-physical system under study. Section 3 and 4 present the failure model used for hurricane characterization and an overview of the survivability model, respectively. In Section 5, we present the evaluation of the survivability model for the cyber-physical system. In Section 6, we give a brief summary of related work. Section 7 contains our conclusions and suggestions for further research.

2 Modeled Power Grid Topology

In this section, we first introduce terminology (Section 2.1) and describe the key features of the smart-grid topology that are used to derive the proposed survivability model (Section 4). In addition, we also introduce storm hardening strategies whose effect is evaluated quantitatively in Section 5.

2.1 Terminology

For the sake of clarity, we define here the key terms used throughout this paper.

- **Wind gust**. The *wind gust* is measured in knots and classified in small, medium, large and catastrophic.
- **Incidence matrix**. Given a physical smart-grid topology, different factors such as the geography of the terrain and the distance from the sea will affect the probability that a given storm will directly hit a section, resulting in the need of manual repair. The *incidence matrix* characterizes, for each section, the wind gust at that section after the occurrence of a storm of a given type.

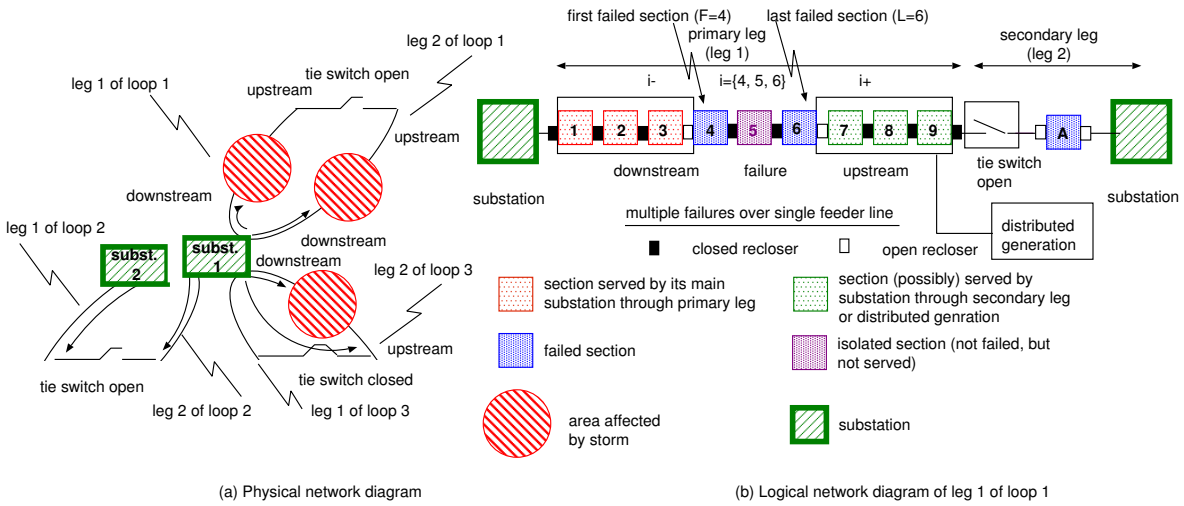

Fig. 1. Physical and logical diagrams of the network topology after the hurricane. Note that in the logical diagram we represent two substations at the two ends of the loop, irrespective of whether they are the same physical substation or different physical substations. In autoloops, as autoloops 1 and 3 in the figure, the two ends of the loop are connected to the same substation. In loop 2, in contrast, the two ends of the loop are connected to different substations.

- **Loop**. The power grid topology is divided in *loops*, which consist of sections. Each loop is connected to a substation at each of its ends.
- **Autoloop**. An autoloop is a special loop that is connected to the same substation at each of its ends. For all practical purposes, in this paper we do not distinguish between loops and autoloops, as the logical network diagrams that are built on top of the physical network diagram are the same for loops and autoloops (see Figure 1). Therefore, we use the terms *loop* and *autoloop* indistinguishably.
- **Legs**. Each loop comprises two *legs*, which are separated by a tie switch. Each leg is a set of contiguous sections: the first section in the leg is directly connected to the substation, and the last section is directly connected to the tie switch. The leg under study is referred to as the *primary leg* and the additional leg of the loop is referred to as the *secondary leg* (the distinction being clear from the context).
- **Tie switch**. The *tie switch* is a switch that controls the flow of energy in a loop. When open, the two separate legs in a loop are fed with energy that flows from the substation up to the tie switch. When the tie switch is closed, the substation feeds energy to the loop through one of its legs, which then relays energy to the other leg.
- **Isolated sections**. The sections in a loop are indexed based on their distance from the substation. After a storm, the set of contiguous sections in a leg between the first and last failed sections are referred to as *isolated sections* (which include the first and last failed sections). The isolated sections will be restored after manual repair.
- **Upstream sections**. The *upstream sections* are the set of contiguous sections farther from the substation, which are not damaged but might be indirectly affected by the storm due to loss of connectivity. The sections in this set are amenable to automatic restoration after the isolated sections are set aside if either (1) distributed generation is available to supply them, or (2) there exists a secondary path from the substation up to the upstream sections, making use of the secondary leg.
- **Downstream sections**. The *downstream sections* are a set of contiguous sections closer to the substation, which are not affected by the storm. The sections in this set are automatically fed by the substation after the isolated sections are set aside.
- **Phased recovery model**. The *phased recovery model* associated with a given leg of a loop is a state machine that characterizes the dynamic state of the leg, from a failure up to full recovery. The transition rates between states, as well as the reward rates associated with each state, depend on the distribution of isolated sections, which in turn depends on the incidence matrix. Although the reward rates and the transition rates of the phased recovery model may vary across legs, the number of states and the possible

transitions between states in the phased recovery model are assumed to be fixed. Fixing the structure of the phased recovery model allows us to pre-compute solutions in a scalable fashion.
- **Reward table**. We associate a set of *reward rates* with each state of the phased recovery model characterizing a given leg. The *reward table* characterizes the expected reward rate (e.g., energy not supplied per time unit) associated with each state for each leg. The expected reward rate depends on the distribution of isolated sections, which in turn depends on the incidence matrix. Note that we use the term *reward rate* even if the corresponding metric of interest represents a cost that should be minimized.

2.2 Con Edison Overhead System in New York

The cyber-physical system under study is based on the Con Edison overhead distribution power grid in New York City and Westchester county, covering an area of 604 square miles. The overhead network consists of 37,000 miles of overhead cable lines that supply power to Westchester County, Staten Island, and parts of the Bronx, Brooklyn, and Queens [27]. The considered power grid includes 154 auto-loops with 219 substations. The 154 auto-loop line feeders are supported structurally by about 284,000 poles and use 47,119 overhead transformers to convert medium voltage (33kV–4kV) to low voltage (120V–240V) supplied to customers [11].

2.3 Hurricane or Tropical Storm Event

Our work is concerned with power distribution network outages that result from a typical hurricane or tropical storm event. We used Hurricane Sandy wind data reported by the U.S. Government National Hurricane Center [13]. Figure 2 shows the maximum wind gusts measured at different locations in New York City and Westchester County, as reported in [13, p.55 et seqq.]. The parts of the Con Edison network that consist of overhead lines are taken from [27] and are shown in light gray. For example, the east and south-east of Queens is predominantly fed by overhead lines, while Manhattan is completely served by an underground network (and thus not considered in this paper).

From this data, we approximate the maximum wind gust at each section required for our model as follows. We derive an interval of observed maximum wind gust for each of the different counties served by the Con Edison overhead network and report these intervals in Table 1. To sample the maximum wind gust at a section, we randomly draw a maximum wind gust speed from the interval associated with the corresponding county.

2.4 Storm Hardening Strategies

The main vulnerability of an overhead distribution system during a typical storm event is wind and tree damage to power distribution and support equipment (e.g., poles, wires, transformers). The storm hardening strategies considered in our model are: (1) undergrounding certain sections of the overhead system, and (2) tree trimming. The utility is deploying several other strategies (e.g., pole hardening) that are out of scope of this work [12]. The overhead distribution system resilience can be improved by replacing portions of the power line with underground equipment. However, due to high cost of undergrounding, the cost effectiveness of the approach needs to be evaluated. The phased recovery model introduced in Section 4 can be used to support such evaluations and to include other less expensive alternatives such as tree trimming.

2.5 Input Data for the Analysis of the Cyber-Physical System

We model the Con Edison overhead distribution power grid by extracting its most important properties as necessary to evaluate the impact of storm events. We model each autoloop as a sequence of sections and we associate each section s (where $s = 1, 2, \ldots, 1542$) with its (1) average load ℓ_s, (2) distributed generation capacity g_s, and (3) maximum wind gust, as shown in Table 1. We allocated to each county a number of loops proportional to the length of overhead distribution power lines in that county (from [27]). The loads in different sections were set based on the load profile benchmark proposed by Rudion *et al.* [29]. The aggregated input data is presented in Table 2.

Table 2 shows that the 154 auto-loops are supplied with 2,276 MW. We assume the distribution of the load among the counties as indicated in the last column of the table. In addition to being supplied by the

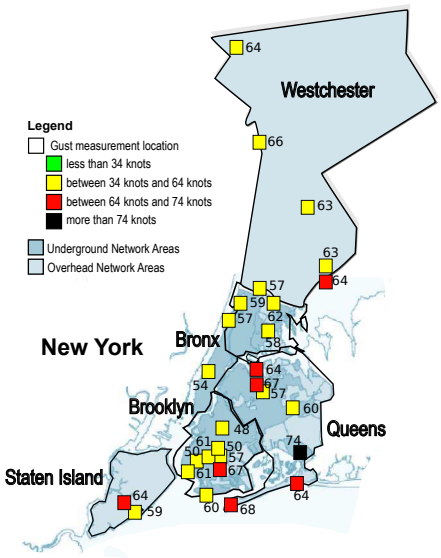

Fig. 2. Wind gust values in knots for Hurricane Sandy. The parts of the Con Edison network that consist of overhead lines are taken from [27].

County	Maximum wind gust intervals (knots)
Brooklyn	[57, 68]
Queens	[60, 74]
Bronx	[57, 62]
Westchester County	[56, 64]
Staten Island	[59, 64]

Table 1. Interval of measured maximum wind gust for locations close to the Con Edison overhead power grid, per county. Maximum wind gust values of sections are sampled from these intervals.

substations, we additionally assume that the auto-loops are also fed by distributed generation from two different renewable energy sources: solar and biomass power systems. For solar, we assume that roughly 30% of the load can be provided by solar generation and distributed irregularly over the sections. For biomass, we assume that 4 biomass generators are available, each producing 20 MW.

County	Loops	Sections	Average load per section (kW)	Average DG per section (kW)	Average net load per section (kW)	Total net load (kW)
Brooklyn	16	158	1,479.33	525.32	954.01	150,734.58
Queens	32	317	1,452.16	375.39	1,076.77	341,335.60
Bronx	12	117	1,500.63	559.83	940.80	110,073.20
Westchester	62	634	1,472.39	435.75	1,036.64	658,267.96
Staten Island	32	317	1,488.01	374.45	1,113.56	352,998.18

Table 2. Model of the Con Edison distribution power grid, including all 154 auto-loops. Each auto-loop comprises a minimum of 8 and a maximum of 12 sections. Net load is the average load minus the load amenable to reduction due to Distributed Generation (DG): the average net load per section (sixth column) is obtained after subtracting the average DG per sections (fifth column) from the average load per section (fourth column).

3 Failure Model

The damage caused by a hurricane at a given section depends on the susceptibility of the section, characterized by the incidence matrix, and the hurricane strength. The susceptibility of the section depends on a number of adjustment factors such as whether the section is underground and trees were trimmed (Table 3). The hurricane strength depends on the geography (see Table 4).

Let W_s be a discrete random variable that characterizes the wind strength level at section s. Table 4 shows the different wind strength levels considered in this paper and the corresponding probabilities of failure $\psi(w)$

Storm hardening	Factor θ
Underground	0.0
Trees trimmed	0.8

Table 3. Adjustment factor θ.

w	Classification	Knots	$\psi(w)$
1	Small	< 34	0.1
2	Medium	$[34, 64)$	0.3
3	Large	$[64, 74)$	0.7
4	Catastrophic	$\geqslant 74$	1.0

Table 4. Probability of failure $\psi(w)$ as a function of wind strength w.

as a function of wind strength w. At each section, the probability of failure must be adjusted to account for the fact that sections are underground and/or trees were trimmed. Let θ_s be the adjustment factor corresponding to section s. The adjustment factors considered in this paper are presented in Table 3.

Let D_s be the random variable that characterizes the state of section $s \in S$ immediately after a failure in leg S. If section s has failed, $D_s = 1$. Otherwise, $D_s = 0$. Then, $P(D_s = 1)$ denotes the probability that s has been damaged by the hurricane and $P(D_s = 0) = 1 - P(D_s = 1)$ denotes the probability that s is still operational. The probability that a section s is directly affected by a storm is given by

$$P(D_s = 1|W_s = w) = \theta_s \psi(w)\,. \tag{1}$$

Given the distribution of wind strengths, we obtain the probability $P(D_s = 1)$ that section s is affected as

$$P(D_s = 1) = \sum_{w=1}^{4} P(D_s = 1|W_s = w)P(W_s = w)\,. \tag{2}$$

Equations (1) and (2) are used in Section 4 to derive key parameters of the survivability model.

4 Survivability Model Overview

In this section, we characterize the principles that have guided the formalization of the recovery procedure, we introduce the assumptions made at design stage, and we present the Markovian and non-Markovian version of the phased recovery model, discussing its properties.

4.1 Modeling Principles

The modeling principles are discussed with reference to the physical and logical diagrams of the network topology after the hurricane passage, which are shown in Figure 1.

State space factorization into legs of loops. We consider the system sectionalized into legs of loops, where each loop is divided into two legs. Each leg is composed of a set of sections, which are separated by reclosers; a leg starts at a substation, and ends at a tie switch.

State aggregation. We aggregate the sections around a failure into upstream sections and downstream sections. The downstream sections are still served through the primary leg. Conversely, the upstream sections are served by the secondary leg, if reachable, or by the distributed generation sources, if available.

Initial state conditioning. We condition the initial state to be a failure state. This allows to avoid dealing with different time scales and characterizing the failure rate.

4.2 Model Properties

The principles followed in the modeling phase as well as the assumptions made on failures and their effects permit to develop a separate survivability model for each loop, sharing the same structure while exposing different parameter values. In so doing, the model structure turns out to be independent of the topology of the power distribution grid, guaranteeing not only simplicity and flexibility of modeling, but also scalability of the overall approach. Moreover, the initial state conditioning permits to characterize the recovery actions given the occurrence of a failure, thus making the model independent of the failure rate.

4.3 Phased Recovery Model

Markovian model. The phased recovery model is characterized by the following states and events. After a section failure, the model is initially in state 0. The sojourn time in state 0 corresponds to the time required for the recloser to isolate the section, which takes an average of $1/\epsilon$ time units. A recloser isolates a section within 10-50 ms after a failure, so in the remainder of this paper we assume $\epsilon = \infty$. Let p be the probability that the communication network is still operational after a section failure, and q be the probability that there is a secondary path to supply energy for sections $i+$. After the isolation of section i is completed, the model transitions to one of following three states:

1. With probability pq the model transitions to state 1, where the distribution network is amenable to automatic restoration.
2. With probability $p(1-q)$ the model transitions to state 3, where the effectiveness of distributed generation will determine if the system is amenable to automatic restoration.
3. With probability $1-p$, the model transitions to state 4, where the communication system requires manual repair, which occurs with rate γ.

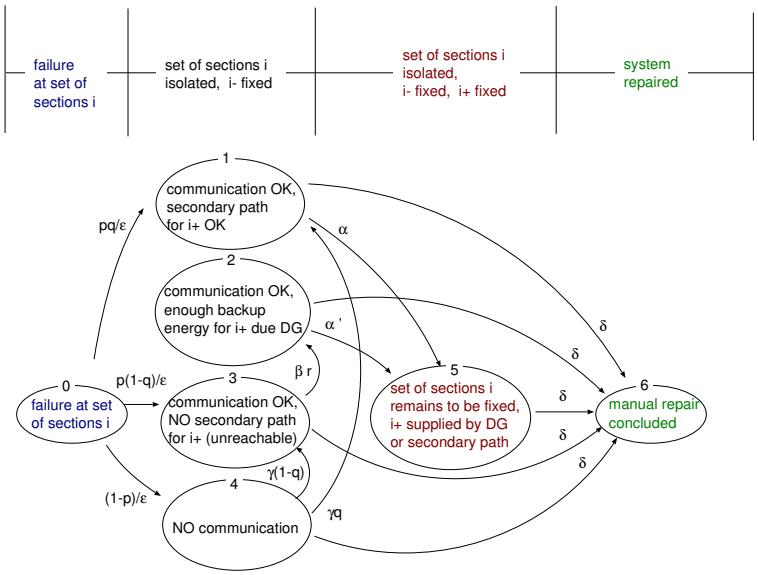

Fig. 3. Markovian phased recovery model.

In state 3, distributed generation is activated after a period of time with average duration $1/\beta$. Let r be the probability that distributed generation can effectively be used. In this case, the model transitions from state 3 to state 2 with rate βr. When the model is in states 1 or 2, the distribution network is amenable to automatic restoration, which occurs after a period of time with average duration $1/\alpha$ and $1/\alpha'$, respectively. A manual repair of section i takes on average $1/\delta$ units of time (and can occur while the system is in states 1-5). After a manual repair, the model transitions to state 6, which corresponds to a fully repaired system.

Non-Markovian model. The phased recovery procedure is modeled through a stochastic Time Petri Net (sTPN) [31,7], which extends Time Petri Nets (TPN) [25] by associating each transition with a Probability Density Function (PDF) supported over its static firing interval and with a weight used to resolve random switches.

A transition is enabled if each of its input places contains a token and none of its inhibitor places contains any tokens. Each enabled transition takes a time-to-fire sampled according to its PDF. We provide here a straightforward description of the sTPN phased recovery model shown in Figure 4, and refer the reader to

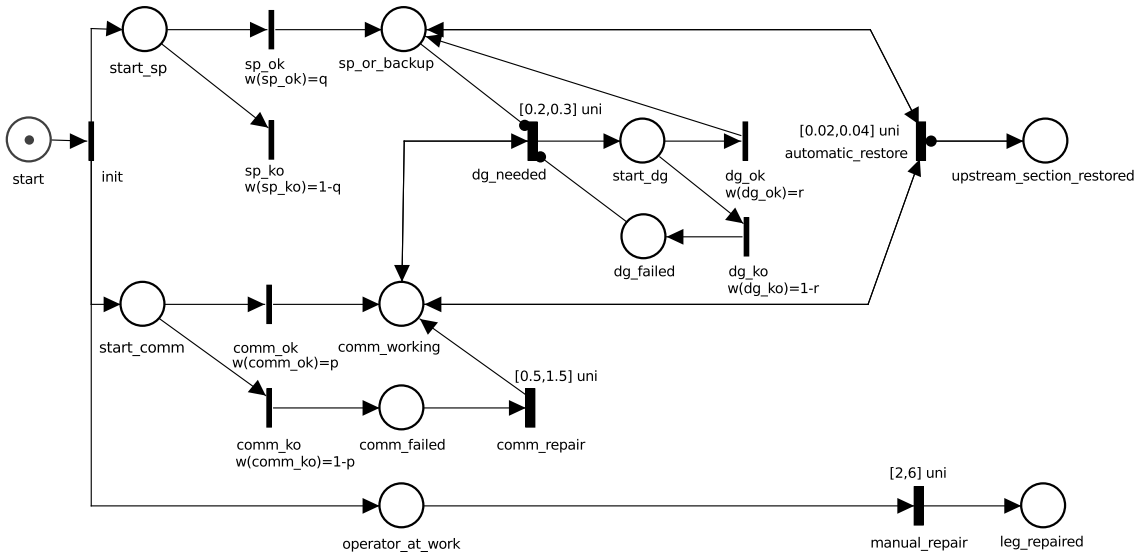

Fig. 4. Non-Markovian phased recovery model. IMM and GEN transitions are represented by thin bars and thick black bars, respectively.

[31,7] for a formal treatment of sTPN syntax and semantics. The specific distributions associated with model transitions refer to the case study analyzed in the experiments.

The immediate (IMM) transition *start* represents the beginning of the recovery procedure (IMM transitions fire in zero time). Its firing enables:

1. The general (GEN) transition *manual_repair*, modeling manual restoration of a set of sections.
2. The IMM transition *comm_ok*, with probability p, accounting for the cases where the communication network is working after a section failure. With probability $1-p$ the communication network is not working after a section failure, which triggers the IMM transition *comm_ko*. When the transition *comm_ko* fires, it enables the GEN transition *comm_repair*, which characterizes the time for restoration of the communication system. After the restoration of the communication system, a token is added to *comm_working*.
3. The IMM transition *sp_ok*, with probability q, accounting for the cases where backup power is sufficient to supply energy to the upstream sections. With probability $1-q$ the backup power does not suffice, which triggers the IMM transition *sp_ko*.

Automatic restoration of upstream sections occurs if the communication network is working and either (1) there is a secondary path to supply for the upstream sections (which fires the *sp_ok* transition, then placing a token in *sp_or_backup*), or (2) distributed generation suffices to supply the upstream sections (which fires the *dg_ok* transition, then placing a token in *sp_or_backup*). In any of these two cases, there will be a token in place *sp_or_backup* and the GEN transition *automatic_restore* will be enabled. After automatic restoration of the upstream sections occurs, the remaining isolated sections must be manually repaired.

Note that the firing of *dg_needed* removes and adds a token to place *comm_working* so as to maintain a token in that place if communication is available, and thus distinguish logical states where communication is up from those where it is down. For the same reason, the firing of *automatic_restore* removes and adds a token to places *comm_working* and *sp_or_backup*. Inhibitor arcs from *sp_or_backup* to *dg_needed* and from *upstream_section_restored* to *automatic_restore* are used to prevent multiple firings of *dg_needed* and *automatic_restore*. All GEN transitions are associated with uniform distributions preserving the mean value of the corresponding EXP distributions in the Markovian model of Figure 3.

The model includes concurrent transitions associated with non-Markovian distributions over possibly bounded supports, which motivates the use of the solution technique proposed in [19] to perform transient stochastic analysis. The approach builds an embedded chain that samples the underlying stochastic process after each firing, maintaining an additional timer that evaluates the time elapsed since the failure event. In Section 5 we use the techniques proposed in [19] and the model presented in Figure 4 to assess storm impact accounting for general residence time distributions in the phased recovery model.

4.4 Parameterization of the Phased Recovery Model

In this section, we characterize the effects of the hurricane on the infrastructure under consideration, which depends on its topology as well as on the characteristics and strength of the hurricane. Together, the infrastructure and the hurricane strength will determine the model parameters p, q, and r.

Disrupted sections. Each leg of the smart grid infrastructure consists of n sections $s_1, \ldots, s_n$. As mentioned in Section 2.1, we consider three regions in an affected leg S: downstream sections, failed sections, and upstream sections. These regions are characterized by the first failed section s_f (section 4 in Figure 1) and the last failed section s_l (section 6 in Figure 1) with $1 \leq f \leq l \leq n$. If no section fails, we set $f = l = 0$.

Probability of available communication. At each loop, the probability of available communication between a substation and the tie switch after the hurricane depends on whether the communication is established through radio, wire, or through the power lines. The value of p depends on the technology adopted for communication, and to capture the different levels of investment we vary p between 0 and 1 in our numerical experiments.

Probability of secondary path available. The probability that a secondary path to restore energy to the upstream sections is available depends on many factors, including the recovery of failed sections. Let Γ' be the indicator random variable that characterizes if the secondary leg is operational. Then,

Definition 1. *The probability that there exists a secondary path to provide energy for the upstream sections after a failure is*

$$q = P(\Gamma' = 1)\,. \tag{3}$$

Leg S includes n sections, i.e., $n = |S|$. Recall that D_s is the random variable that characterizes the state of section $s \in S$ immediately after a failure in leg S for $s = 1, 2, \ldots, n$. If section s has failed, $D_s = 1$; otherwise, $D_s = 0$ (see Section 3). Furthermore, let S' be the other leg (secondary path) in the current loop, with n' sections, that might be used to provide energy for the upstream sections of S. In this paper, to simplify the presentation, we assume that all sections fail independently. This is clearly a simplifying assumption, which can be relaxed without compromising the general methodology presented in this work.

Then, the probability that the secondary path to the failed region in S is operational is

$$q = \prod_{s' \in S'} P(D_{s'} = 0)\,. \tag{4}$$

Table 5 summarizes the notation used throughout this paper.

Characterizing isolated sections. Next, our goal is to characterize the set of sections that are isolated from the network due to failures. We order the sections in a leg increasingly as a function of their distance from the substation. In what follows, we refer to the *first* and *last* failed sections in a leg with respect to that order. Let F be the index of the first failed section in S (see Figure 1). Then, the probability that the first failed section is section f is given by

$$P(F = f) = \begin{cases} P(D_f = 1) \prod_{j=1}^{f-1} P(D_j = 0) & \text{if } f > 0, \\ \prod_{j=1}^{n} P(D_j = 0) & \text{if } f = 0. \end{cases} \tag{5}$$

Equation (5) indicates that section f is the first failed section in the leg if it is damaged ($D_f = 1$) and the sections before section f have not been affected ($D_j = 0$ for $j = 1, \ldots, f-1$). Note that if the hurricane did not affect any section in the leg, $F = 0$, which occurs when $D_j = 0$ for $j = 1, \ldots, n$.

Let L be the index of the last failed section in S. Then, the probability that the last failed section is section l is given by

$$P(L = l) = \sum_{f=0}^{n} P(L = l | F = f) P(F = f) \tag{6}$$

Variable	Description
p	probability that communication is working after failure
q	probability that there is a secondary path to upstream sections
r	probability that distributed generation suffices to provide for upstream
$\mathcal{S}_u$	average energy supplied per time-unit at state u of the phased recovery model
F	index of the first failed section
L	index of the last failed section
n	number of sections in primary leg, $n = \|S\|$
S	set of sections in primary leg
S'	set of sections in secondary leg
Γ'	indicator random variable, equals 1 if secondary path is available
$\mathcal{I}$	set of contiguous sections between first and last failed section (including them)
$\mathcal{I}+$	set of upstream sections
$\mathcal{I}-$	set of downstream sections
D_j	indicator random variable, equals 1 if section j failed
ℓ_j	load at section j
g_j	distributed generation at section j
$\mathcal{U}(l)$	upstream surplus when last failed section is section l

Table 5. Table of notation. All variables are a function of the leg under study, which must be clear from the context.

where

$$P(L = l|F = f) = \begin{cases} P(D_l = 1)\prod_{j=l+1}^{n} P(D_j = 0) & \text{if } f > 0 \text{ and } l > f, \\ \prod_{j=l+1}^{n} P(D_j = 0) & \text{if } f > 0 \text{ and } l = f, \\ 1 & \text{if } f = l = 0, \\ 0 & \text{otherwise,} \end{cases} \tag{7}$$

with the convention that $\prod_{j=m}^{n} P(D_j = 0) = 1$ if $m > n$. According to Eq. (7), section l is the last failed section in the leg if it is damaged ($D_l = 1$) and the sections after section l have not been affected ($D_j = 0$ for $j = l + 1, \ldots, n$). If the hurricane affects only section f in the leg, then $F = L = f$, which occurs if section f is the first failed section and the sections afterwards have not been affected ($D_j = 0$ for $j = l + 1, \ldots, n$). Note that, if the hurricane did not affect any section in the leg, $F = 0$, which implies that $L = 0$.

Rewards. Let ℓ_s denote the average load at section s. Next, our goal is to determine the average energy not supplied after a failure.

States 1, 2, 3, 4. Let $\mathcal{S}_u$ be the energy supplied per time unit when the phased recovery model is in state u, $1 \le u \le 4$. Then, the expected energy supplied per unit time, in state u, is given by

$$E[\mathcal{S}_u] = \sum_{f=0}^{n} E[\mathcal{S}_u|F = f]P(F = f) \tag{8}$$

where, for $1 \le u \le 4$,

$$E[\mathcal{S}_u|F = f] = \begin{cases} \sum_{1\le j<f} \ell_j \text{ if } f > 0, \\ \sum_{1\le j\le n} \ell_j \text{ if } f = 0. \end{cases} \tag{9}$$

Equation (9) indicates that the expected energy supplied at states 1-4 is the total load supplied to the downstream sections in case failures occur (see Figure 1), and is the total demanded load otherwise.

State 5. Next, our goal is to compute the expected energy supplied in state 5 of the phased recovery model. To this aim, we consider two cases, depending on whether the secondary leg is operational. Recall that $q = P(\Gamma' = 1)$ is the probability that the secondary leg is operational. Then, conditioning on whether the

secondary leg is operational in state 5 of the phased recovery model, the expected energy supplied per time unit is given by

$$E[\mathcal{S}_5] = E[\mathcal{S}_5|\Gamma' = 1]\, q + E[\mathcal{S}_5|\Gamma' = 0]\,(1-q)\,. \tag{10}$$

In what follows, we compute $E[\mathcal{S}_5|\Gamma' = 1]$ and $E[\mathcal{S}_5|\Gamma' = 0]$. The expected energy supplied in state 5 of the phased recovery model, given that a secondary path is available, is given by

$$E[\mathcal{S}_5|\Gamma' = 1] = \sum_{0\le f\le n} \sum_{0\le l\le n} E[\mathcal{S}_5|F = f, L = l, \Gamma' = 1] P(L = l|F = f, \Gamma' = 1) P(F = f|\Gamma' = 1) \tag{11}$$

where $P(L = l|F = f, \Gamma' = 1)$ and $P(F = f|\Gamma' = 1)$ are given by Eqs. (7) and (5), respectively, and $E[\mathcal{S}_5|F = f, L = l, \Gamma' = 1]$ is given by

$$E[\mathcal{S}_5|F = f, L = l, \Gamma' = 1] = \sum_{1\le j<f} \ell_j + \sum_{l<j\le n} \ell_j\,. \tag{12}$$

Next, we compute $E[\mathcal{S}_5|\Gamma' = 0]$. Let g_s denote the average distributed energy generated at section s.

Definition 2. *Let $\mathcal{U}(l)$ be the surplus generation at the upstream of the current leg when $L = l$,*

$$\mathcal{U}(l) = \sum_{l<j\le n} (g_j - \ell_j)\,. \tag{13}$$

Once a storm hits a leg of a loop, we assume that the leg is broken into *isolated sections*, *upstream sections* and *downstream sections* (see Section 3). The isolated sections are restored through manual repair, and energy is supplied to them only after manual repair concludes. Upstream sections, in contrast, are amenable to automatic restoration through Distributed Generation (DG) or making use of a secondary path (secondary leg). We do not consider isolated restoration of sections within the failed region, i.e., we assume that either there is enough backup energy from distributed generation to supply to the upstream sections (in which case they will be automatically recovered), or distributed generation will not be used. In addition, we only consider distributed generation capacities up to the tie switch.

If the surplus generation is zero or positive, the upstream sections can be restored using distributed generation, even if the secondary leg is not operational.

Definition 3. *The probability r of whether DG can restore the isolated upstream sections is*

$$r = \sum_{1<l\le n} 1_{\mathcal{U}(l)>0} P(L = l) \tag{14}$$

where

$$1_{\mathcal{U}(l)>0} = \begin{cases} 1 & \text{if } \mathcal{U}(l) > 0, \\ 0 & \text{otherwise.} \end{cases} \tag{15}$$

The expected energy supplied in state 5 of the phased recovery model, given that a secondary path is not available, is given by

$$E[\mathcal{S}_5|\Gamma' = 0] = \sum_{1<l\le n} P(L = l|\Gamma' = 0) E[\mathcal{S}_5|L = l, \Gamma' = 0] \tag{16}$$

where

$$E[\mathcal{S}_5|L = l, \Gamma' = 0] = \begin{cases} \sum_{l<j\le n} \ell_j & \text{if } \mathcal{U}(l) \ge 0, \\ 0 & \text{otherwise.} \end{cases} \tag{17}$$

Equation (17) indicates that the expected energy supplied, given that a secondary path is not available, is equal to the energy load of the upstream sections in case DG suffices. Replacing Eqs. (11) and (16) into Eq. (10), we obtain the expected energy supplied in state 5 of the phased recovery model. To simplify the presentation, in the remainder of this paper, when evaluating Eq. (16) we will additionally assume that the probability $P(L = l)$ that l is the last failed section in the primary leg is independent of whether the secondary leg is available, i.e., $P(L = l|\Gamma' = 0) = P(L = l)$.

State 6. In state 6, the expected energy supplied equals the total system load, and is given by

$$E[\mathcal{S}_6] = \sum_{1 \le j \le |S|} \ell_j \,. \tag{18}$$

Summary. Table 6 summarizes the results presented in this section. It shows how the probabilities and reward rates of different states of the phased recovery model are computed, and their meaning.

State	Reward rate	Equations
1-4	Energy supplied per unit time to downstream sections	(8)–(9)
5	Energy supplied per unit time to downstream and upstream sections	(10)–(17)
6	Energy supplied per unit time to whole system	(18)

Variable	Event probability	Equations
q	There is a secondary path to upstream sections	(3)–(4)
r	Distributed generation suffices for upstream	(14)–(15)

Table 6. Summary of probabilities and reward rate semantics and expressions.

5 Evaluation

In this section, we present the results from the analysis of the Con Edison network described in Section 2. Section 5.1 illustrates the investment options under evaluation, the experimental setup, and information on the execution. Section 5.2 presents the results of Markovian and non-Markovian analysis.

5.1 Setup and Execution

To analyze the survivability of the Con Edison network N, we both derive the parameters and solve the survivability models described in Section 4 separately for each autoloop $S \in N$. The survivability models yield the expected energy not supplied at each point in time for each autoloop. To aggregate the results, we sum up the expected energy not supplied at each point in time over all considered autoloops. As an additional metric, we consider the Accumulated Expected Energy Not Supplied (AEENS) until system recovery.

In order to evaluate the ability of the proposed approach to quantify storm hardening strategies, we consider three different investment strategies and quantify their effect on the expected energy not supplied:

1. *Investment strategy 1 (INV1): Trim the trees along all sections.* Under this investment strategy, we multiply the failure probability of each section by the "trees trimmed" adjustment factor $\theta = 0.8$ (see Table 3).
2. *Investment strategy 2 (INV2): For each autoloop, place the first section and the last section underground.* Under this investment strategy, we set the failure probability of each section neighboring the substation to zero (adjustment factor $\theta = 0$, see Table 3).
3. *Investment strategy 3 (INV3): Combine strategies 1 and 2.* Under this investment strategy, we set the probability of each section neighboring the substation to zero and multiply the failure probability of the remaining sections by the "trees trimmed" adjustment factor $\theta = 0.8$.

All investment options in place reduce the failure probability of some or all sections and thus affect the rewards of the model as well as the probabilities q and r. In the base model, we expect 575 sections to fail as a result of $\sum_{S \in N} \sum_{s \in S} P(D_s = 1)$. For the investment options, the expected number of failed sections is reduced to 460 (INV1), 458 (INV2), and 366 (INV3).

Investment	State 1	State 2	State 3	State 4	State 5	State 6
None	7.4936	7.4936	7.4936	7.4936	6.6600	0
INV1	6.5089	6.5089	6.5089	6.5089	5.2990	0
INV2	6.3918	6.3918	6.3918	6.3918	5.1499	0
INV3	5.5224	5.5224	5.5224	5.5224	3.9104	0

Table 7. Rewards in kW averaged over all legs of all autoloops, for each investment option.

Investment	Sections with $r = 0$	Sections with $r > 0$	Average of r over sections with $r > 0$	Sections with $q = 0$	Sections with $q > 0$	Average of q over sections with $q > 0$
None	298	14	0.159	18	294	0.094
INV1	296	16	0.157	0	312	0.139
INV2	298	14	0.186	20	292	0.140
INV3	296	16	0.183	0	312	0.190

Table 8. For parameters r and q and each investment option, the number of sections with parameter equal to zero, greater than zero, and the average value over sections with parameter greater than zero.

Table 7 shows the average rewards for each state over all autoloops. Note that this is averaged over all autoloops, while we actually solve the model separately for each autoloop. Thus, the different states of the models are not reached at the same time for different autoloops. Table 8 characterizes the parameters r and q over all legs of all autoloops. We use expert knowledge to set the different model parameters. We let the mean manual repair time be 4 hours ($\delta = 1/4$) and the mean automatic repair time be 2 minutes ($\alpha = \alpha' = 30$). Distributed generation takes an average of 15 minutes to be activated ($\beta = 4$) and communication takes an average of 1 hour to be repaired ($\gamma = 1$). Throughout the evaluation, we let $p = 0.5$. We implemented the reward calculations and the calculation of parameters q and r in Matlab as described in Section 4.4.

Deriving the rewards for the case study setup takes about 5 seconds on a commercial off-the-shelf machine. The solution of the Markovian model was implemented in Matlab as well, and solving the Markovian phased recovery model takes about 10 seconds. Using the recent release of the ORIS Tool based on the Sirio framework [8,9,6], regenerative transient analysis of the non-Markovian phased recovery model up to time 16 h can be performed in nearly 3 seconds with a time step of 0.1 h. Evaluating the EENS of the non-Markovian model takes roughly 15 minutes for each investment option.

We assumed an infinite number of repair trucks and repair teams, i.e., we assumed that the mean manual repair time $1/\delta$ of each autoloop is independent of the number of overall failures. This is a simplifying assumption that we will relax in future work.

Note that loops operate autonomously from each other as far as distribution automation features are concerned. There might be dependencies between loop repair times due to geographical closeness, global availability of required resources, and so on. The geographical closeness was taken into account by analyzing the wind gusts per location. Nevertheless, the analysis of manual repair times as a function of geographical closeness and number of trucks available is out of scope of the paper.

5.2 Evaluation results

Table 9 shows the accumulated EENS until the complete system recovery for the base network and the three investment options.

Investment option			
None	INV1	INV2	INV3
4.5862	3.7915	3.8762	3.1268

Table 9. Accumulated EENS in gigawatt (GW) until complete system recovery for different investment options.

Figure 5 shows the results for the EENS over time for the base network with no investment (red) and the three networks resulting from the three investment strategies (blue, green, black). The first four curves in the figure key are the results of the Markovian analysis and have the typical exponential form. The fifth to eighth curves are the results of the non-Markovian analysis; the EENS value at time zero is the same as in Markovian analysis. With both solution approaches, the base model has the highest EENS at all points in

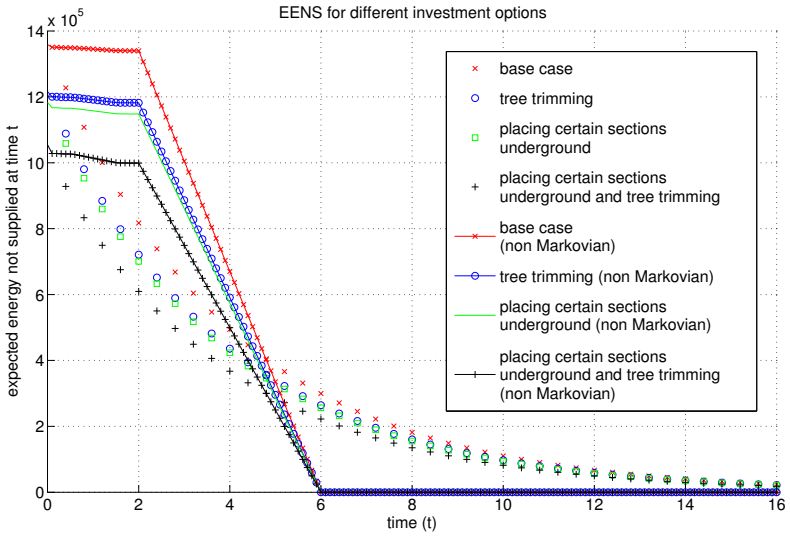

Fig. 5. Expected energy not supplied over time: base network and different investment options.

time. Investment strategy 2 (some sections underground) performs slightly better than investment strategy 1 (trim trees) for the considered setup. Combining the two strategies, i.e., strategy 3, yields the best results.

Comparing the behavior of the EENS over time, we observe that the non-Markovian EENS results have a different behavior, exactly reaching a null value at time 6 h; this corresponds to the completion of the manual repair, which is uniformly distributed over the bounded support $[2, 6]$ h. Before time 2 h, the decrease of the EENS rate is due to the repair of upstream sections; given the low probability that distributed generation is sufficient to provide energy to upstream sections (r parameter), the expected reduction is limited and the overall dynamics is dominated by the manual recovery operation. Different investment options are distinguished more significantly by guaranteeing different initial EENS immediately after a failure.

The results demonstrate how our models can be used to quantitatively assess investment options for storm hardening of distribution grids. Note that the numerical results of our analysis are by no means general recipes for the suitability of storm hardening strategies. Instead, for each power network under study, each considered storm scenario, and each set of storm hardening investment options, the input data (cf. Section 2) has to be determined and fed into our tool chain to quantify the effects of storm hardening strategies. Then, the calculation of the survivability parametrization and the solution of the survivability models can be done automatically by our tools.

6 Related Work

Survivability models of distribution automation power grids were first introduced in [2,21,24,1]. These models were solved analytically using multiple techniques, such as transient analysis of Markov chains, state aggregation, and hierarchical modeling.

In [1], a Continuous Time Markov Chain (CTMC) is used to model the actions taken in reaction to a failure in a telecommunication network, evaluating an extension of the System Average Interruption Duration Index (SAIDI) that accounts for variations of energy demand and supply during a multi-step recovery process. The approach is extended in [2] to quantify the Energy Not Supplied (ENS) in the presence of multiple failures under specific independence assumptions. Stochastic Activity Networks (SANs) [30] are used in [3] to model the operation of large critical infrastructures, encompassing interdependencies among them and applying

Monte Carlo simulation to evaluate the distribution of cascade sizes. Hierarchical composition is exploited in [23] to merge the expressiveness of state-based Markov reward models with the computational efficiency of combinatorial methods, deriving transient availability and performability measures for telecommunication systems.

Unit commitment scheduling for coordination of energy demand and supply is studied in [5]. The authors model renewable energy resources through Hidden Markov Models (HMMs) [28] and power demand loads as a Markov-Modulated Poisson Process (MMPP) [14]. The problem is formulated as a partially observable Markov decision process and a distributed scheme is presented such that the most suitable generation unit is dynamically scheduled based on system parameters including demand loads, utility costs, reliability, and pollution emissions of generation units. In [10], a probabilistic model checker based on the PRISM tool [22] is developed and used to evaluate demand-side management in micro-grids. The authors consider a decentralized infrastructure which allows users to oversee demand while dissuading them from abuse and incentivizing cooperation among them. The approach leverages the model of turn-based stochastic multi-player games, where players can either collaborate or compete to achieve a specific goal, and is used to detect potential weaknesses and unexpected behaviors in smart energy management algorithms.

The approach of [16,17] discusses elementary mechanisms for distributed run-time control of power grids with a substantial share of renewable energy sources (especially photovoltaic power generators), which make electric power production much more subject to unpredictable and significant fluctuations. To this end, non-Markovian models specified in MODEST [4] are used to evaluate production control algorithms and demand-side mechanisms, especially in terms of stability, availability, quality of service, and fairness.

Heegaard and Trivedi [18] study the survivability of the Internet and computer networks. Similarities between the operation of the Internet and the working principles of future power grids are leveraged in [15] to support design of distributed and decentralized power grid control appliances. Keshav and Rosenberg [20] also point out how concepts pioneered by the Internet are applicable to the design of smart grids.

The papers mentioned above are related to ours as they consider the survivability of critical infrastructures. Nonetheless, the work presented here significantly differs from previous work as we (1) combine the survivability model with a model to characterize a hurricane, (2) propose a scalable way to assess the survivability of large infrastructures, and (3) consider and compare investment options that have not been analyzed before using survivability models.

7 Conclusion

In this paper, we have introduced an innovative approach to model failures and recoveries resulting from large hurricanes. To this end, a scalable survivability model has been developed to assess the evolution of the failure recovery process on a real distribution automation network. More specifically, we have used as a case study Hurricane Sandy impacts on the overhead distribution of New York metropolitan region.

We have created a scalable survivability model based on a phase-recovery Markov chain with rewards. The reward rates characterize metrics such as the expected energy not supplied per time unit. They are parameterized using information about the geography and the network topology. Our model can be evaluated efficiently because each distribution loop is modeled independently by a separate phased recovery Markov chain. We have also developed a non-Markovian phased recovery model that allowed us to better approximate repair distributions. We have presented evaluations of the Markovian and non-Markovian phased recovery models and we are encouraged by the efficiency at which we obtained our initial results.

As topics for further research, we envision the development of heuristics to evaluate investment alternatives for distribution automation reliability improvement, by assessing customer affecting metrics such as energy not supplied up to full system recovery. The validation to specific environments requires engagement of the target utilities and possible model refinements. The proposed model is general enough to allow for topology generalizations and to incorporate historical data from different environments.

References

1. Alberto Avritzer, Sindhu Suresh, Daniel Sadoc Menasché, Rosa Maria Meri Leão, Edmundo de Souza e Silva, Morganna Carmem Diniz, Kishor Trivedi, Lucia Happe, and Anne Koziolek. Survivability models for the assessment of smart grid distribution automation network designs. In *Proceedings of the International Conference on Performance Engineering*, pages 241–252. ACM, 2013.

2. Alberto Avritzer, Sindhu Suresh, Daniel Sadoc Menasché, Rosa Maria Meri Leão, Edmundo de Souza e Silva, Morganna Carmem Diniz, Kishor Trivedi, Lucia Happe, and Anne Koziolek. Survivability models for the assessment of smart grid distribution automation network designs. *Concurrency and Computation Practice and Experience*, 2014.
3. Robin E. Bloomfield, Lubos Buzna, Peter Popov, Kizito Salako, and David Wright. Stochastic modelling of the effects of interdependencies between critical infrastructure. In *CRITIS*, pages 201–212, 2009.
4. Henrik C. Bohnenkamp, Pedro R. D'Argenio, Holger Hermanns, and Joost-Pieter Katoen. Modest: A compositional modeling formalism for hard and softly timed systems. *IEEE Trans. Softw. Eng.*, 32(10):812–830, 2006.
5. Shengrong Bu, F Richard Yu, and Peter X Liu. Stochastic unit commitment in smart grid communications. In *Computer Communications Workshop, 2011 IEEE Conference on*, pages 307–312. IEEE, 2011.
6. G. Bucci, L. Carnevali, L. Ridi, and E. Vicario. Oris: a tool for modeling, verification and evaluation of real-time systems. *Int. Journal of SW Tools for Technology Transfer*, 12(5):391 – 403, 2010.
7. L. Carnevali, L. Grassi, and E. Vicario. State-Density Functions over DBM Domains in the Analysis of Non-Markovian Models. *IEEE Trans. on Software Engineering*, 35(2):178–194, 2009.
8. L. Carnevali, L. Ridi, and E. Vicario. A framework for simulation and symbolic state space analysis of non-Markovian models. In *SAFECOMP*, pages 409–422, 2011.
9. L. Carnevali, L. Ridi, and E. Vicario. Sirio: A framework for simulation and symbolic state space analysis of non-Markovian models. In *QEST '11*, pages 153–154, 2011.
10. Taolue Chen, Vojtech Forejt, Marta Z. Kwiatkowska, David Parker, and Aistis Simaitis. Automatic verification of competitive stochastic systems. *Formal Methods in System Design*, 43(1):61–92, 2013.
11. Consolidated Edison of New York, Inc. *Report on the preparation and system restoration performance.* Jan 2013.
12. Consolidated Edison of New York, Inc. *Storm Hardening and Resiliency Collaborative Report.* Dec. 2013.
13. E. S. Blake et. al. *Tropical Cyclone Report - Hurricane Sandy (AL182012).* Nat'l Hurricane Center, Feb. 2013.
14. Wolfgang Fischer and Kathleen Meier-Hellstern. The markov-modulated poisson process (mmpp) cookbook. *Performance Evaluation*, 18(2):149–171, 1993.
15. Ernst Moritz Hahn, Arnd Hartmanns, Holger Hermanns, and Joost-Pieter Katoen. A compositional modelling and analysis framework for stochastic hybrid systems. *Formal Methods in System Design*, 43(2):191–232, 2013.
16. Arnd Hartmanns and Holger Hermanns. Modelling and decentralised runtime control of self-stabilising power micro grids. In *ISoLA (1)*, pages 420–439, 2012.
17. Arnd Hartmanns, Holger Hermanns, and Pascal Berrang. A comparative analysis of decentralized power grid stabilization strategies. In *Winter Simulation Conference*, page 158, 2012.
18. P. E. Heegaard and K. S. Trivedi. Network survivability modeling. *Computer Networks*, 53(8):1215–1234, 2009.
19. András Horváth, Marco Paolieri, Lorenzo Ridi, and Enrico Vicario. Transient analysis of non-markovian models using stochastic state classes. *Performance Evaluation*, 69(7):315–335, 2012.
20. Srinivasan Keshav and Catherine Rosenberg. How internet concepts and technologies can help green and smarten the electrical grid. *ACM SIGCOMM Computer Communication Review*, 2011.
21. A. Koziolek, L. Happe, A. Avritzer, and S. Suresh. A common analysis framework for smart distribution networks applied to survivability analysis of distribution automation. In *Software Engineering for the Smart Grid (SE4SG), 2012 International Workshop on*, pages 23 –29, june 2012.
22. Marta Z. Kwiatkowska, Gethin Norman, and David Parker. Prism 4.0: Verification of probabilistic real-time systems. In *CAV*, pages 585–591, 2011.
23. M. Lanus, Liang Yin, and K.S. Trivedi. Hierarchical composition and aggregation of state-based availability and performability models. *Reliability, IEEE Transactions on*, 52(1):44–52, 2003.
24. D. Menasché, R. M. M. Leão, E. de Souza e Silva, A. Avritzer, S. Suresh, K. Trivedi, R. A. Marie, L. Happe, and A. Koziolek. Survivability analysis of power distribution in smart grids with active and reactive power modeling. In *GreenMetrics Workshop*, 2012.
25. P. Merlin and D.J. Farber. Recoverability of communication protocols. *IEEE Trans. on Comm.*, 24(9):1036–1043, 1976.
26. NYC Department of Environmental Protection, Fred Gliesing, CF. Challenges to westchester's forests.
27. Office of Long-Term Planning and Sustainability, City of New York. *Utilization of Underground and Overhead Power Lines in the City of New York.* City of New York, December 2013.
28. Lawrence Rabiner and Biing-Hwang Juang. An introduction to hidden markov models. *ASSP Magazine, IEEE*, 3(1):4–16, 1986.
29. K. Rudion, A. Orths, Z.A. Styczynski, and K. Strunz. Design of benchmark of medium voltage distribution network for investigation of dg integration. In *Power Engineering Society General Meeting, 2006. IEEE*, 2006.
30. William H. Sanders and John F. Meyer. Stochastic activity networks: Formal definitions and concepts. In *European Educational Forum: School on Formal Methods and Performance Analysis*, pages 315–343, 2000.
31. E. Vicario, L. Sassoli, and L. Carnevali. Using stochastic state classes in quantitative evaluation of dense-time reactive systems. *IEEE Trans. on Software Engineering*, 35(5):703–719, 2009.